

Document downloaded from:

<http://hdl.handle.net/10251/78355>

This paper must be cited as:

López Molina, JA.; Rivera Ortun, MJ.; Berjano Zanón, E. (2017). Analytical transient-time solution for temperature in non perfused tissue during radiofrequency ablation. *Applied Mathematical Modelling*. 42:618-635. doi:10.1016/j.apm.2016.10.044.



The final publication is available at

<http://dx.doi.org/10.1016/j.apm.2016.10.044>

Copyright Elsevier

Additional Information

# Analytical transient-time solution for temperature in non perfused tissue during radiofrequency ablation

Juan A. López Molina<sup>1</sup>, María J. Rivera<sup>1</sup>, Enrique Berjano<sup>2,3</sup>

## Abstract

Radiofrequency ablation (RFA) with internally cooled needle-like electrodes is a technique widely used to destroy cancer cells. In a previous study we obtained the analytical solution of the biological heat equation associated with the RFA problem in perfused tissue, i.e. when the governing equation which models the temperature distribution in tissue includes the blood perfusion term. We also found that under these circumstances the temperature profiles always reach a steady state (limit temperature). However, the analytical solution of the RFA thermal problem without perfusion (e.g. conducted on an organ in which atraumatic vascular clamping is performed to temporarily interrupt blood perfusion), cannot be directly obtained by setting the blood perfusion term to zero in the previously obtained solution. In fact, it is necessary to address the mathematical resolution in a totally different way. Our goal was to obtain the analytical expression of the temperature distribution in an RFA process with internally cooled needle-like electrodes when the biological tissue is not perfused. We consider two spatial domains: A finite domain which represents the real situation, and an infinite domain, which only makes sense from a mathematical point of view and which has been traditionally employed in analytical studies. Even though considering infinite time is not realistic, these approaches are surely worth considering in order to understand what happens "far from the electrode" or for "very long periods of time." The results indicate that the temperature value is finite both when the spatial domain is finite (which implies that a steady state is reached), and when time is finite for any spatial domain. From this it can be concluded that a steady state is never reached if the spatial domain is infinite.

---

<sup>1</sup>Applied Mathematics Department, Universitat Politècnica de València, Valencia, Spain

<sup>2</sup>Biomedical Synergy, Electronic Engineering Department, Universitat Politècnica de València, Valencia, Spain

<sup>3</sup>Address for correspondence: Dr. Enrique Berjano, Electronic Engineering Department, Universitat Politècnica de València, Camino de Vera, 46022 Valencia, Spain. E-mail: eberjano@eln.upv.es

# 1 Introduction

Radiofrequency ablation (RFA) is a high-temperature ablative technique which raises tissue temperature over  $50^{\circ}\text{C}$  with the aim of irreversibly destroying the target tissue. Different electrode designs have been clinically used for this purpose, including needle-like electrodes and, especially, internally cooled electrodes which have been broadly employed in several medical techniques such as tumor ablation [1]. Internal cooling makes it possible to keep the temperature at the electrode surface more or less constant, hence avoiding tissue sticking and increasing lesions size. The objective of using an RF applicator to treat tumors is to create the largest possible thermal lesion. The idea behind this is that the thermal lesion (volume with temperatures  $> 50^{\circ}\text{C}$ ) should completely enclose the tumor, and consequently the larger the thermal lesion, the larger the tumor that can be treated.

In order to investigate the electrical-thermal performance during RFA, theoretical models with an analytical solution have previously been proposed [2]-[6]. In a previous study we developed a theoretical model of an internally cooled needle-like electrode for RFA based on a cylindrical geometry and solved the transit-time thermal problem in an analytical way [7]. In particular, we considered the bioheat equation, which is the governing equation in the case of perfused tissues, i.e. where the blood perfusion term is included. We found that under this condition the temperature profiles in the tissue always reached a steady state (limit temperature). Now we are interested in obtaining an analytical expression for the temperature distribution in the case of a non perfused tissue. In a clinical setting, this scenario would be that of RFA in an organ in which atraumatic vascular clamping is performed to temporarily interrupt blood perfusion. This maneuver (known as the Pringle maneuver) allows larger thermal lesion and hence bigger tumors can be treated [8]. Since the analytical solution under this condition cannot be directly obtained by setting the blood perfusion term of the solution previously obtained to zero, we have had to address the mathematical problem in a totally different way. An intensive use of Bessel functions was required to do this, thus the non elementary properties used in the analytical calculations are given in the Appendix.

# 2 Methods

Figure 1 shows the real shape of an internally cooled needle-like electrode used for RF ablation, and how the electrode can be modeled by simplifying the scenario and considering an ideal conductor with infinite length totally inserted in a homogeneous tissue. Then in cylindrical coordinates we assume that in every point the temperature  $T$  only depends of the time  $t$  and the distance  $r$  to the axis of the electrode. The governing thermal equation to study RF ablation can be the bioheat

equation [9]:

$$\eta c \frac{\partial T}{\partial t} = \nabla \cdot (k \nabla T) + S - \eta_b c_b \omega_b (T - T_b) \quad (1)$$

where  $\eta$ ,  $c$  and  $k$  are the density, specific heat and thermal conductivity of the tissue respectively,  $\eta_b$ ,  $c_b$  and  $\omega_b$  are the density, specific heat and perfusion coefficient of the blood,  $T_b$  is the blood temperature and  $S$  represents the heat sources. The last term on the right side of Eq. (1) is the blood perfusion term. Since our interest is to deal with non perfused tissues, this term will be ignored. Assuming all quantities  $\eta$ ,  $\eta_b$ ,  $c$ ,  $c_b$  and  $k$  to be constant and that the heat source is independent on the polar angle  $\theta$  and working in cylindrical coordinates  $(r, \theta)$  the equation (1) becomes

$$\eta c \frac{\partial T}{\partial t}(r, t) = k \left( \frac{\partial^2 T}{\partial r^2}(r, t) + \frac{1}{r} \frac{\partial T}{\partial r}(r, t) \right) + S(r, t). \quad (2)$$

The heat source (S) in this case is the dissipated electrical power density ( $W/m^3$ ) into the tissue. Due to the cylindrical geometry of the theoretical model, we employed the same formulation used by Haemmerich et al [3], and hence we have:

$$\eta c \frac{\partial T}{\partial t}(r, t) = k \left( \frac{\partial^2 T}{\partial r^2}(r, t) + \frac{1}{r} \frac{\partial T}{\partial r}(r, t) \right) + \frac{j_0^2 r_0^2}{\sigma r^2} \quad (3)$$

where  $j_0$  is the density current at the conductor surface,  $\sigma$  is the electrical conductivity and  $r_0$  is the electrode radius.

We change to dimensionless variables

$$\rho = \frac{r}{r_0}, \quad \xi = \frac{\alpha t}{r_0^2} \quad V(\rho, \xi) = \frac{\sigma k}{j_0^2 r_0^2} \left( T \left( r_0 \rho, \frac{r_0^2 \xi}{\alpha} \right) - T_0 \right)$$

(where  $T_0$  is the body temperature (which has the same value as blood temperature), and  $\alpha = \frac{k}{c\eta}$ ) which leads us to the problem

$$- \left( \frac{\partial^2 V}{\partial \rho^2} + \frac{1}{\rho} \frac{\partial V}{\partial \rho} \right) + \frac{\partial V}{\partial \xi} = \frac{1}{\rho^2} \quad (4)$$

## 3 Results

### 3.1 Finite spatial domain

In this subsection we present the analytical solution  $T_R(r, t)$  of (3) in the case in which the boundary condition is at a finite distance  $R$  from the axis of the electrode. The initial and boundary conditions of an internally cooled electrode are

$$T_R(r, 0) = T_0 \quad \forall r_0 < r < R \quad (5)$$

$$T_R(r_0, t) = T_C \quad \forall t > 0 \quad (6)$$

$$T_R(R, t) = T_0 \quad \forall t > 0 \quad (7)$$

In dimensionless variable, we wish to solve  $V_R(\rho, \xi)$  in the boundary value problem

$$-\left(\frac{\partial^2 V_R}{\partial \rho^2} + \frac{1}{\rho} \frac{\partial V_R}{\partial \rho}\right) + \frac{\partial V_R}{\partial \xi} = \frac{1}{\rho^2} \quad \forall (\rho, \xi) \in ]1, R/r_0[ \times ]0, \infty[ \quad (8)$$

$$V_R(1, \xi) = \frac{\sigma k(T_C - T_b)}{j_0^2 r_0^2} := (-B) \quad \forall \xi > 0 \quad (9)$$

$$V_R(R/r_0, \xi) = 0 \quad \forall \xi > 0 \quad (10)$$

$$V_R(\rho, 0) = 0 \quad \forall \rho \in ]1, R/r_0[ \quad (11)$$

We express the solution of this problem as

$$V_R(\rho, \xi) = W_R(\rho, \xi) + W_{R,S}(\rho) \quad (12)$$

where  $W_R(\rho, \xi)$  and  $W_{R,S}(\rho)$  are the solutions of the boundary value problems

$$-\left(W_{R,S}''(\rho) + \frac{1}{\rho} W_{R,S}'(\rho)\right) = \frac{1}{\rho^2} \quad (13)$$

$$W_{R,S}(1, \xi) = -B \quad \forall \xi > 0 \quad (14)$$

$$W_{R,S}(R/r_0, \xi) = 0 \quad \forall \xi > 0 \quad (15)$$

and

$$-\left(\frac{\partial^2 W_R}{\partial \rho^2} + \frac{1}{\rho} \frac{\partial W_R}{\partial \rho}\right) + \frac{\partial W_R}{\partial \xi} = 0 \quad \forall (\rho, \xi) \in ]1, R/r_0[ \times ]0, \infty[ \quad (16)$$

$$W_R(1, \xi) = W_R(R/r_0, \xi) = 0 \quad \forall \xi > 0, \quad (17)$$

and the initial condition

$$W_R(\rho, 0) = -W_{R,S}(\rho) \quad \forall \rho \in ]1, R/r_0[. \quad (18)$$

(Dirichlet boundary condition).

The solution of (13), (14), (15) was obtained in [12]:

$$W_{R,S}(\rho) = -B + \left(\frac{B}{\log \frac{R}{r_0}} + \frac{1}{2} \log \frac{R}{r_0}\right) \log \rho - \frac{1}{2} \log^2 \rho. \quad (19)$$

To solve (16), (17), (18) we use the classical method of separation of variables. After standard steps, we obtain

$$W_R(\rho, \xi) = \sum_{m=1}^{\infty} A_m e^{-\lambda_m^2 \xi} \left( J_0(\lambda_m \rho) - \frac{J_0(\lambda_m)}{Y_0(\lambda_m)} Y_0(\lambda_m \rho) \right) \quad (20)$$

where

$$A_m = \frac{\int_1^{\frac{R}{r_0}} -W_{R,S}(\rho) \rho \left( J_0(\lambda_m \rho) - \frac{J_0(\lambda_m)}{Y_0(\lambda_m)} Y_0(\lambda_m \rho) \right) d\rho}{\int_1^{\frac{R}{r_0}} \rho \left( J_0(\lambda_m \rho) - \frac{J_0(\lambda_m)}{Y_0(\lambda_m)} Y_0(\lambda_m \rho) \right)^2 d\rho}$$

and  $\{\lambda_m\}_{m=1}^{\infty}$  is the sequence of positive roots of the equation  $J_0(\lambda)Y_0(\lambda R/r_0) = J_0(\lambda R/r_0)Y_0(\lambda)$ . It is important to note that  $\lim_{\xi \rightarrow \infty} V_R(\rho, \xi) = W_{R,S}(\rho)$ . Then the limit temperature coincides with  $W_{R,S}(\rho)$ .

### 3.2 Infinite spatial domain

In this case the initial and boundary conditions are

$$T(r, 0) = T_0 \quad \forall r > r_0 \quad (21)$$

$$T(r_0, t) = T_C \quad \forall t > 0 \quad (22)$$

$$\lim_{r \rightarrow \infty} T(r, t) = T_0 \quad \forall t > 0 \quad (23)$$

Then in dimensionless variable, we wish to solve the boundary value problem

$$-\left( \frac{\partial^2 V}{\partial \rho^2} + \frac{1}{\rho} \frac{\partial V}{\partial \rho} \right) + \frac{\partial V}{\partial \xi} = \frac{1}{\rho^2} \quad \forall (\rho, \xi) \in ]1, \infty[ \times ]0, \infty[ \quad (24)$$

$$V(\rho, 0) = 0 \quad \forall \rho > 1 \quad (25)$$

$$\lim_{\rho \rightarrow \infty} V(\rho, \xi) = 0 \quad \forall \xi > 0 \quad (26)$$

$$V(1, \xi) = \frac{\sigma k(T_C - T_b)}{j_0^2 r_0^2} := (-B) \quad (27)$$

The solution of this problem was presented in [7], but there the blood perfusion term was included, that is  $\omega_b \neq 0$ , and in dimensionless variables with  $\beta := \frac{\eta_b c_b \omega_b r_0^2}{k} \neq 0$ . In this case taking the Laplace transform  $D(\rho, s, \beta) := \mathcal{L}[V(\rho, \xi)](\rho, s, \beta)$  with respect to  $\xi$ , the problem is

$$\rho^2 \frac{d^2 D}{d\rho^2} + \rho \frac{dD}{d\rho} - (s + \beta) \rho^2 D = -\frac{1}{s} \quad (28)$$

$$\lim_{\rho \rightarrow \infty} D(\rho, s, \beta) = 0 \quad (29)$$

$$D(1, s, \beta) = -\frac{B}{s} \quad (30)$$

and its solution was

$$\begin{aligned}
D(\rho, s, \beta) &= \frac{1}{s} I_0(\rho\sqrt{s+\beta}) \int_{\rho}^{\infty} \frac{K_0(v\sqrt{s+\beta})}{v} dv \\
&+ \frac{1}{s} K_0(\rho\sqrt{s+\beta}) \int_1^{\rho} \frac{I_0(v\sqrt{s+\beta})}{v} dv - B \frac{K_0(\rho\sqrt{s+\beta})}{s K_0(\sqrt{s+\beta})} \\
&- I_0(\sqrt{s+\beta}) \frac{K_0(\rho\sqrt{s+\beta})}{s K_0(\sqrt{s+\beta})} \int_1^{\infty} \frac{K_0(v\sqrt{s+\beta})}{v} dv. \tag{31}
\end{aligned}$$

In our case taking  $\beta = 0$  in (31) the Laplace transform  $\mathfrak{L}[V(\rho, \xi)](\rho, s, 0)$  is

$$\begin{aligned}
D(\rho, s, 0) &= \frac{1}{s} I_0(\rho\sqrt{s}) \int_{\rho}^{\infty} \frac{K_0(v\sqrt{s})}{v} dv + \frac{1}{s} K_0(\rho\sqrt{s}) \int_1^{\rho} \frac{I_0(v\sqrt{s})}{v} dv \\
&- B \frac{K_0(\rho\sqrt{s})}{s K_0(\sqrt{s})} - I_0(\sqrt{s}) \frac{K_0(\rho\sqrt{s})}{s K_0(\sqrt{s})} \int_1^{\infty} \frac{K_0(v\sqrt{s})}{v} dv. \tag{32}
\end{aligned}$$

In the inversion process of (31), it was crucial that  $\beta \neq 0$  because in that case  $s = 0$  is not a branch point of  $D(\rho, s, \beta)$  (Fig. 2-A), while in the case  $\beta = 0$ ,  $D(\rho, s, 0)$  has a branch point in  $s = 0$  (Fig. 2-B) and so the previous results [7] cannot be transformed in a formally direct way. We hence need to perform a direct inversion of (32), which is presented in Results section.

To find the inverse Laplace transform of (32) it is convenient to rewrite the expression of  $D(\rho, \xi) := D(\rho, \xi, 0)$  in the way

$$D(\rho, s, 0) = \int_{\rho}^{\infty} \frac{G_1(\rho, s, v)}{v} dv + \int_1^{\rho} \frac{G_2(\rho, s, v)}{v} dv - \int_1^{\rho} \frac{G_3(\rho, s, v)}{v} dv - B G_4(\rho, s) \tag{33}$$

where we have defined

$$\begin{aligned}
G_1(\rho, s, v) &:= \frac{K_0(v\sqrt{s})}{s} \left( I_0(\rho\sqrt{s}) - I_0(\sqrt{s}) \frac{K_0(\rho\sqrt{s})}{K_0(\sqrt{s})} \right), \\
G_2(\rho, s, v) &:= \frac{1}{s} K_0(\rho\sqrt{s}) I_0(v\sqrt{s}), \\
G_3(\rho, s, v) &:= I_0(\sqrt{s}) \frac{K_0(\rho\sqrt{s})}{K_0(\sqrt{s})} \frac{K_0(v\sqrt{s})}{s} \quad \text{and} \quad G_4(\rho, s) := \frac{K_0(\rho\sqrt{s})}{s K_0(\sqrt{s})}.
\end{aligned}$$

Let  $T \subset \mathbb{R}$ . For  $j = 1, 2, 3$ , if  $\mathfrak{L}^{-1}[G_j(\rho, s, v)](\rho, \xi, v)$  is integrable in  $T$  with respect to the  $v$ -variable, by Fubini's theorem we will have

$$\mathfrak{L} \left[ \int_T \mathfrak{L}^{-1} \left[ \frac{G_j}{v} \right] (\rho, \xi, v) dv \right] (\rho, \xi) = \int_0^{\infty} e^{-s\xi} \left( \int_T \mathfrak{L}^{-1} \left[ \frac{G_j}{v} \right] (\rho, \xi, v) dv \right) d\xi =$$

$$= \int_T \mathfrak{L} \left[ \mathfrak{L}^{-1} \left[ \frac{G_j}{v} \right] (\rho, \xi, v) \right] (\rho, s, v) dv = \int_T \frac{G_j(\rho, \xi, v)}{v} dv$$

and, consequently,

$$\mathfrak{L}^{-1} \left[ \int_T \frac{G_j(\rho, \xi, v)}{v} dv \right] (\rho, \xi) = \int_T \mathfrak{L}^{-1} \left[ \frac{G_j}{v} \right] (\rho, \xi, v) dv. \quad (34)$$

It follows that the method we shall use to find  $\mathfrak{L}^{-1}[D(\rho, s, 0)]$  will be to compute  $\mathfrak{L}^{-1}[\frac{G_j}{v}](\rho, s, v), j = 1, 2, 3$ , next to check its integrability with respect to  $v$  in the corresponding intervals and to find  $\mathfrak{L}^{-1}[G_4](\rho, s, v)$  and then to apply the formula

$$\begin{aligned} \mathfrak{L}^{-1}[D(\rho, s, 0)](\rho, \xi) &= \int_{\rho}^{\infty} \mathfrak{L}^{-1} \left[ \frac{G_1}{v} \right] (\rho, \xi, v) dv + \\ &+ \int_1^{\rho} \mathfrak{L}^{-1} \left[ \frac{G_2}{v} \right] (\rho, \xi, v) dv - \int_1^{\infty} \mathfrak{L}^{-1} \left[ \frac{G_3}{v} \right] (\rho, \xi, v) dv - B \mathfrak{L}^{-1}[G_4](\rho, \xi). \end{aligned} \quad (35)$$

Each  $G_j(\rho, s, v), 1 \leq j \leq 4$ , considered as a function of the complex variable  $s$  has a branch point at  $s = 0$ . So the natural way to find  $\mathfrak{L}^{-1}[G_j](\rho, \xi, v)$  is by using Bromwich's formula along the contour of Figure 2-B. We shall always use the principal value of  $Arg(z) \in ] - \pi, \pi[$  and define  $\mathcal{D}_0 := \mathbb{C} \setminus ] - \infty, 0]$ .

The branch point  $s = 0$  and the factor  $\frac{1}{s}$  appearing in the expression of  $G_j(\rho, s, v)$  will be the cause of many complications in the inversion process which leads us to direct and very subtle computations. For instance, if we deal with  $\mathfrak{L}^{-1}[G_1](\rho, \xi, v)$ , by (63) and L'Hôpital's rule we find easily that in  $\mathcal{D}_0$

$$\lim_{s \rightarrow 0} \frac{K_0(v\sqrt{s})}{K_0(\sqrt{s})} = \lim_{s \rightarrow 0} \frac{\log \frac{v\sqrt{s}}{2}}{\log \frac{\sqrt{s}}{2}} = 1 \quad (36)$$

and once again using (63)

$$\begin{aligned} &\lim_{s \rightarrow 0} K_0(v\sqrt{s}) \left( I_0(\rho\sqrt{s}) - I_0(\sqrt{s}) \frac{K_0(\rho\sqrt{s})}{K_0(\sqrt{s})} \right) = \\ &= \lim_{s \rightarrow 0} \frac{K_0(v\sqrt{s})}{K_0(\sqrt{s})} \left( I_0(\rho\sqrt{s})K_0(\sqrt{s}) - I_0(\sqrt{s})K_0(\rho\sqrt{s}) \right) = \\ &= \lim_{s \rightarrow 0} \left( -I_0(\rho\sqrt{s})I_0(\sqrt{s}) \log \frac{\sqrt{s}}{2} + I_0(\sqrt{s})I_0(\rho\sqrt{s}) \log \frac{\rho\sqrt{s}}{2} \right) = \\ &= \lim_{s \rightarrow 0} I_0(\rho\sqrt{s})I_0(\sqrt{s}) \log \frac{\rho\sqrt{s}}{\frac{\sqrt{s}}{2}} = \log \rho. \end{aligned} \quad (37)$$



That means that the integrals along  $L_1$  and  $L_2$  in Figure 2-B which appear in a direct application of Bromwich's formula will be divergent at  $s = 0$ . Indeed the sum of the contributions of both curvilinear integrals (which will be twice the integral along  $L_1$  of the imaginary part of  $G_1(\rho, s, v)$ ) is not certain to be convergent. The same problem will appear working with  $\mathfrak{L}^{-1}[G_j](\rho, \xi, v), j = 2, 3, 4$  and so we need a total modification of the method used in the case  $\beta \neq 0$ .

The main idea is to fix a number  $\frac{1}{2} < \alpha < 1$  and to consider the functions  $H_j(\rho, s, v) = s G_j(\rho, s, v), 1 \leq j \leq 4$ . By the convolution theorem we will have

$$\mathfrak{L}^{-1}[G_j](\rho, \xi, v) = \mathfrak{L}^{-1} \left[ \frac{1}{s^{1-\alpha}} \frac{1}{s^\alpha} H_j \right] = \frac{\xi^{-\alpha}}{\Gamma(1-\alpha)} * \mathfrak{L}^{-1} \left[ \frac{1}{s^\alpha} H_j \right] (\rho, \xi, v)$$

(where  $*$  denotes the convolution product) and our task will be to find  $g_j(\rho, \xi, v, \alpha) := \mathfrak{L}^{-1} \left[ \frac{H_j}{s^\alpha} \right] (\rho, \xi, v)$ , for each  $j = 1, 2, 3, 4$  and every  $\frac{1}{2} < \alpha < 1$ . As  $\mathfrak{L}^{-1}[G_j](\rho, \xi, v)$  is clearly independent of  $\alpha$ , there must exist  $\lim_{\alpha \rightarrow \frac{1}{2}} g_j(\rho, \xi, v, \alpha)$  and we will eliminate the presence of  $\alpha$  taking limits when  $\alpha \rightarrow \frac{1}{2}$ . As  $\Gamma(1/2) = \sqrt{\pi}$  we finally obtain

$$\mathfrak{L}^{-1}[G_j](\rho, \xi, v) = \lim_{\alpha \rightarrow \frac{1}{2}} \frac{1}{\sqrt{\pi}} \int_0^\xi \frac{g_j(\rho, w, v, \alpha)}{\sqrt{\xi-w}} dw = \frac{1}{\sqrt{\pi}} \int_0^\xi \frac{g_j(\rho, w, v, \frac{1}{2})}{\sqrt{\xi-w}} dw \quad (38)$$

provided that  $g_j(\rho, w, v, \alpha)$  is right continuous at  $\alpha = \frac{1}{2}$  and the integral (38) is convergent.

### 3.2.1 Computation of $\mathfrak{L}^{-1}[G_1](\rho, \xi, v)$

Now  $H_1(s, \rho, v) = K_0(v\sqrt{s})E(s, \rho)$  where

$$E(s, \rho) := I_0(\rho\sqrt{s}) - I_0(\sqrt{s}) \frac{K_0(\rho\sqrt{s})}{K_0(\sqrt{s})}.$$

If  $Im(s) > 0$ ,  $s \in \mathcal{D}_0$ ,  $Re(s) \leq \gamma_0$  and  $|s|$  is large enough, using the asymptotic expansions (73) and (71) we find  $C_1 > 0, C_2 > 0$  independent of  $s$  such that

$$\left| \frac{K_0(\rho\sqrt{s})}{K_0(\sqrt{s})} \right| \leq \frac{C_1}{\sqrt{\rho}} \left| e^{-(\rho-1)\sqrt{s}} \right|$$

and

$$\begin{aligned} & \left| \frac{K_0(v\sqrt{s})}{s^\alpha} E(s, \rho) \right| \leq \\ & \leq \frac{C_2}{\sqrt[4]{v\rho}|s|^{\alpha+\frac{1}{2}}} \left( \left| e^{-(v-\rho)\sqrt{s}} \right| + \left| e^{-(v+\rho)\sqrt{s}} \right| + \left| e^{-(v+\rho-2)\sqrt{s}} \right| + \left| e^{-(v+\rho)\sqrt{s}} \right| \right) = \end{aligned}$$

$$\begin{aligned}
&= \frac{C_2}{\sqrt[4]{v\rho}|s|^{\alpha+\frac{1}{2}}} \left( e^{-(v-\rho)\sqrt{|s|}\cos\frac{\text{Arg } s}{2}} + e^{-(v+\rho)\sqrt{|s|}\cos\frac{\text{Arg } s}{2}} \right. \\
&\quad \left. + e^{-(v+\rho-2)\sqrt{|s|}\cos\frac{\text{Arg } s}{2}} + e^{-(v+\rho)\sqrt{|s|}\cos\frac{\text{Arg } s}{2}} \right) \leq \frac{4 C_2}{\sqrt[4]{v\rho}|s|^{\alpha+\frac{1}{2}}} \quad (39)
\end{aligned}$$

because  $v \geq \rho \geq 1$  and  $\cos\frac{\text{Arg } s}{2} \geq 0$ . A similar result holds for  $\text{Im}(s) \leq 0$  and  $|s|$  is large enough using (73) and (72). Since  $\frac{1}{2} < \alpha < 1$ , Bromwich's contour of figure 2-B can be used to find  $\mathfrak{L}[G_1](\rho, \xi, v)$ .

Moreover, by (37) we have

$$\lim_{s \rightarrow 0} s \frac{e^{s\xi} K_0(v\sqrt{s})}{s^\alpha} E(s, \rho) = 0$$

and since the function to be inverted has no singular point inside Bromwich's contour ([10], section 15.7), by Bromwich's formula, (39) and Jordan's lemma the residues theorem gives us

$$\begin{aligned}
g_1(\rho, w, v, \alpha) &= \mathfrak{L}^{-1} \left[ \frac{H_1}{s^\alpha} \right] (\rho, \xi, v) = \mathfrak{L}^{-1} \left[ \frac{K_0(v\sqrt{s})}{s^\alpha} E(s, \rho, v) \right] (\rho, \xi, v) = \\
&= \frac{1}{2\pi i} \lim_{R \rightarrow \infty, \varepsilon \rightarrow 0} \left( - \int_{L_1} \frac{e^{s\xi} K_0(v\sqrt{s})}{s^\alpha} E(s, \rho, v) ds - \int_{L_2} \frac{e^{s\xi} K_0(v\sqrt{s})}{s^\alpha} E(s, \rho, v) ds \right) =
\end{aligned}$$

and as  $J_0(z)$  is an even function of  $z$ , by (65), (64) and (66)

$$\begin{aligned}
&= \frac{-1}{2} \text{Im} \int_{-\infty}^0 \frac{e^{s\xi} (J_0(v\sqrt{-s}) i + Y_0(v\sqrt{-s}))}{(-s)^\alpha e^{\alpha\pi i}} (J_0(\rho\sqrt{-s}) \\
&\quad - J_0(\sqrt{-s}) \frac{J_0(\rho\sqrt{-s}) i + Y_0(\rho\sqrt{-s})}{J_0(\sqrt{-s}) i + Y_0(\sqrt{-s})}) ds =
\end{aligned}$$

and after elementary operations and the change  $x = -s$

$$= \frac{1}{2} \int_0^\infty \frac{e^{-x\xi}}{x^\alpha} \left( J_0(\rho\sqrt{x}) A_1(x, \alpha) - J_0(\sqrt{x}) \frac{A_2(x, \alpha) A_3(x) + A_4(x, \alpha) A_5(x)}{J_0^2(\sqrt{x}) + Y_0^2(\sqrt{x})} \right) dx \quad (40)$$

where

$$\begin{aligned}
A_1(x, \alpha) &:= \cos(\alpha\pi) J_0(v\sqrt{x}) - \sin(\alpha\pi) Y_0(v\sqrt{x}), \\
A_2(x, \alpha) &:= \cos(\alpha\pi) Y_0(v\sqrt{x}) + \sin(\alpha\pi) J_0(v\sqrt{x}), \\
A_3(x) &:= J_0(\rho\sqrt{x}) Y_0(\sqrt{x}) - J_0(\sqrt{x}) Y_0(\rho\sqrt{x}), \\
A_4(x, \alpha) &:= \cos(\alpha\pi) J_0(v\sqrt{x}) - \sin(\alpha\pi) Y_0(v\sqrt{x})
\end{aligned}$$

and

$$A_5(x) := Y_0(\rho\sqrt{x})Y_0(\sqrt{x}) + J_0(\sqrt{x})J_0(\rho\sqrt{x}).$$

The integral (40) is indeed uniformly convergent for  $\alpha \in [\frac{1}{2}, \frac{3}{4}[$  since (Weierstrass's criterion) by (59), (67) and (68) there are constants  $C_3(\rho, v) > 0, C_4(\rho) > 0$  such that

$$\forall \alpha \in \left[\frac{1}{2}, \frac{3}{4}\right[ \quad |g_1(\rho, \xi, v, \alpha)| \leq C_3(\rho, v) \int_0^1 \frac{dx}{x^{\frac{3}{4} + \frac{1}{8}}} + C_4(\rho) \int_1^\infty \frac{e^{-x\xi}}{x^{\frac{1}{2}}} dx$$

and these two integrals are clearly convergent. It follows that  $g_1(\rho, \xi, v, \alpha)$  is a right continuous function of  $\alpha$  at  $\alpha = \frac{1}{2}$  and by (38) and (40)

$$\begin{aligned} \mathfrak{L}^{-1}[G_1](\rho, \xi, v) &= \frac{1}{\sqrt{\pi}} \int_0^\xi \frac{g_1(\rho, w, v, \frac{1}{2})}{\sqrt{\xi - w}} dw = \\ &= \frac{1}{2\sqrt{\pi}} \int_0^\infty \left( \int_0^\xi \frac{e^{-xw}}{\sqrt{\xi - w}} dw \right) \frac{1}{\sqrt{x}} \left( -Y_0(v\sqrt{x})J_0(\rho\sqrt{x}) \right. \\ &\quad \left. + Y_0(v\sqrt{x})J_0(\sqrt{x}) \frac{J_0(\rho\sqrt{x})J_0(\sqrt{x}) + Y_0(\sqrt{x})Y_0(\rho\sqrt{x})}{J_0^2(\sqrt{x}) + Y_0^2(\sqrt{x})} \right. \\ &\quad \left. - J_0(v\sqrt{x})J_0(\sqrt{x}) \frac{J_0(\rho\sqrt{x})Y_0(\sqrt{x}) - J_0(\sqrt{x})Y_0(\rho\sqrt{x})}{J_0^2(\sqrt{x}) + Y_0^2(\sqrt{x})} \right) dx. \end{aligned}$$

It follows easily from (67), (68), and (70) that for every  $\rho \geq 1$  there is  $C_5(\rho) > 0$  such that

$$\begin{aligned} &\left| \frac{\mathfrak{L}^{-1}[G_1](\rho, \xi, v)}{v} \right| \leq \\ &\leq \frac{\sqrt{\xi}}{\sqrt{\pi}} \int_0^\infty \frac{1}{v\sqrt{x}} \left( \int_0^\xi \frac{e^{-xw}}{\sqrt{\xi - w}} dw \right) \left( \frac{2}{\pi\sqrt{v\rho x}} + O\left(\frac{1}{\rho x^{\frac{3}{4}}\sqrt{v}}\right) \right. \\ &\quad \left. + \left( \frac{2}{\pi\sqrt{vx}} + O\left(\frac{1}{x^{\frac{3}{4}}\sqrt{v}}\right) \right) C_5(\rho) \right) dx \end{aligned}$$

which is of the order  $v^{-\frac{3}{2}}$  when  $v \rightarrow \infty$  and so ensures the convergence of

$$\int_\rho^\infty \frac{\mathfrak{L}^{-1}[G_1](\rho, \xi, v)}{v} dv.$$

### 3.2.2 Computation of $\mathfrak{L}^{-1}[G_2](\rho, \xi, v)$

To find

$$\int_1^\rho \frac{\mathfrak{L}^{-1}[G_2](\rho, \xi, v)}{v} dv$$

we have  $\rho \geq v \geq 1$ . Then, by the asymptotic expansions (73), (71), for  $|s|$  large enough,  $s \in \mathcal{D}_0$ ,  $Im(s) \geq 0$  and  $Re(s) \leq \gamma_0$ , for every  $\frac{1}{2} < \alpha < 1$ , there is  $C_6 > 0$  such that

$$\begin{aligned} \left| \frac{1}{s^\alpha} K_0(\rho\sqrt{s}) I_0(v\sqrt{s}) \right| &\leq \frac{C_6}{|s|^\alpha} \left| \sqrt{\frac{1}{\rho\sqrt{s}}} e^{-\rho\sqrt{s}} \right| \left( \left| \frac{e^{v\sqrt{s}}}{\sqrt{v\sqrt{s}}} \right| + \left| \frac{e^{-v\sqrt{s}}}{\sqrt{v\sqrt{s}}} \right| \right) = \\ &= \frac{C_6}{|s|^{\alpha+\frac{1}{2}} \sqrt{\rho v}} \left( e^{-(\rho-v)\sqrt{|s|} \cos(\frac{Arg s}{2})} + e^{-(\rho+v)\sqrt{|s|} \cos(\frac{Arg s}{2})} \right) \leq \frac{2 C_6}{\sqrt{\rho v} |s|^{\alpha+\frac{1}{2}}} \end{aligned} \quad (41)$$

since  $\cos(\frac{Arg s}{2}) \geq 0$ . A similar result holds if  $Im(s) < 0$  using (72). As  $\alpha + \frac{1}{2} > 1$  actually we can use Bromwich's contour of figure 2-B to find  $\mathfrak{L}^{-1} \left[ \frac{H_3}{s^\alpha} \right](\rho, \xi, v)$ . Noting that (59) and (63) gives us for every  $\alpha \in [\frac{1}{2}, 1[$

$$\lim_{s \rightarrow 0, s \in \mathcal{D}_0} s e^{s\xi} \frac{K_0(v\sqrt{s})}{s^\alpha} I_0(\rho\sqrt{s}) = \lim_{s \rightarrow 0} s^{1-\alpha} (-I_0(v\sqrt{s}) \log \frac{v\sqrt{s}}{2} + Z(v\sqrt{s})) = 0 \quad (42)$$

and that  $g_2(\rho, \xi, v, \alpha)$  has no singular point inside the contour of Bromwich, from (41), Jordan's lemma and Bromwich's formula and the theorem of residues we obtain

$$\begin{aligned} g_2(\rho, \xi, v, \alpha) &= \mathfrak{L}^{-1} \left[ \frac{1}{s^\alpha} K_0(v\sqrt{s}) I_0(\rho\sqrt{s}) \right](\rho, \xi, v) = \\ &= \lim_{R \rightarrow -\infty, \varepsilon \rightarrow 0} \frac{-1}{2\pi i} \left( \int_{L_1} \frac{e^{s\xi}}{s^\alpha} K_0(v\sqrt{s}) I_0(\rho\sqrt{s}) ds + \int_{L_2} \frac{e^{s\xi}}{s^\alpha} K_0(v\sqrt{s}) I_0(\rho\sqrt{s}) ds \right) = \end{aligned}$$

and since  $J_0(z)$  is an even function, by (63) and (66)

$$= \frac{1}{2} Im \int_{-\infty}^0 e^{s\xi} J_0(\rho\sqrt{-s}) \frac{J_0(v\sqrt{-s})i + Y_0(v\sqrt{-s})}{(-s)^\alpha e^{\alpha\pi i}} ds =$$

and after the change  $-s = x$

$$= \frac{1}{2} \int_0^\infty \frac{e^{-x\xi}}{x^\alpha} J_0(\rho\sqrt{x}) (\cos(\alpha\pi) J_0(v\sqrt{x}) - \sin(\alpha\pi) Y_0(v\sqrt{x})) dx. \quad (43)$$

With the same argument used in subsection 3.2.1 it is shown that (43) is an improper integral which is uniformly convergent for  $\alpha \in [\frac{1}{2}, \frac{3}{4}[$ . Then  $g_2(\rho, \xi, v, \alpha)$  is right continuous at  $\alpha = \frac{1}{2}$  and by (38) and Fubini's theorem

$$\mathfrak{L}^{-1}[G_2](\rho, \xi, v) = \frac{1}{\sqrt{\pi}} \int_0^\xi \frac{g_2(\rho, w, v, \frac{1}{2})}{\sqrt{\xi - w}} dw =$$

$$= -\frac{1}{2\sqrt{\pi}} \int_0^\infty \left( \int_0^\xi \frac{e^{-xw}}{\sqrt{\xi-w}} dw \right) \frac{J_0(\rho\sqrt{x})Y_0(v\sqrt{x})}{\sqrt{x}} dx.$$

### 3.2.3 Computation of $\mathfrak{L}^{-1}[G_3](\rho, \xi, v)$

Noting that to find

$$\int_1^\rho \frac{\mathfrak{L}^{-1}[G_3](\rho, \xi, v)}{v} dv$$

we have  $\rho \geq v \geq 1$ , we can proceed in the same way that in subsection 3.2.1 in order to obtain suitable estimations of

$$f(s, \rho, v) := I_0(\sqrt{s})K_0(\rho\sqrt{s}) \frac{K_0(v\sqrt{s})}{s^\alpha K_0(\sqrt{s})}$$

when  $s \in \mathcal{D}_0$ ,  $|s| \rightarrow \infty$ ,  $Re(s) \leq \gamma_0$  and  $\frac{1}{2} < \alpha < 1$ , which allows us to use once again Bromwich's contour of figure 2. Note that actually  $f(s, \rho, v)$  appear in the second summand of  $H_1(s, \rho, v)$  and we can use the results in subsection 3.2.1. We obtain

$$\begin{aligned} \mathfrak{L}^{-1}[G_3](\rho, \xi, v) &= \frac{1}{\sqrt{\pi}} \int_0^\xi \frac{g_3(\rho, w, v, \frac{1}{2})}{\sqrt{\xi-w}} dw = \\ &= \frac{1}{2\sqrt{\pi}} \int_0^\infty \left( \int_0^\xi \frac{e^{-xw}}{\sqrt{\xi-w}} dw \right) \left( -Y_0(v\sqrt{x})J_0(\sqrt{x}) \frac{J_0(\rho\sqrt{x})J_0(\sqrt{x}) + Y_0(\sqrt{x})Y_0(\rho\sqrt{x})}{\sqrt{x}(J_0^2(\sqrt{x}) + Y_0^2(\sqrt{x}))} \right. \\ &\quad \left. + J_0(v\sqrt{x})J_0(\sqrt{x}) \frac{J_0(\rho\sqrt{x})Y_0(\sqrt{x}) - J_0(\sqrt{x})Y_0(\rho\sqrt{x})}{\sqrt{x}(J_0^2(\sqrt{x}) + Y_0^2(\sqrt{x}))} \right) dx. \end{aligned}$$

### 3.2.4 Computation of $\mathfrak{L}^{-1}[G_4](\rho, \xi, v)$

In the computation of

$$g_4(\rho, \xi, v, \alpha) = \mathfrak{L}^{-1} \left[ \frac{H_2(\rho, s, v)}{s^\alpha} \right] = \mathfrak{L}^{-1} \left[ \frac{1}{s^\alpha} \frac{K_0(\rho\sqrt{s})}{K_0(\sqrt{s})} \right]$$

a new complication arises: in order to use Bromwich's formula, by the asymptotic expansion (73) we have for  $Re(s) \leq \gamma_0$  and  $|s|$  large enough

$$\left| \frac{1}{s^\alpha} \frac{K_0(\rho\sqrt{s})}{K_0(\sqrt{s})} \right| = \left| \frac{1}{s^\alpha} \frac{\sqrt{\frac{\pi}{2\rho\sqrt{s}}} e^{-\rho\sqrt{s}} \left( 1 + O\left(\frac{1}{\rho\sqrt{s}}\right) \right)}{\sqrt{\frac{\pi}{2\sqrt{s}}} e^{-\sqrt{s}} \left( 1 + O\left(\frac{1}{\sqrt{s}}\right) \right)} \right| \leq 3 \left| \frac{e^{-(\rho-1)\sqrt{s}}}{\sqrt{\rho} s^\alpha} \right| \leq \frac{3}{|s|^\alpha} \quad (44)$$

(because  $\cos \frac{Arg s}{2} > 0$ ). As  $\alpha < 1$  the employment of Bromwich's formula is not assured. On the other hand we can not to divide by  $s$  in order to use the formula of the Laplace transform of a primitive since

$$\lim_{s \rightarrow 0} s \frac{K_0(\rho\sqrt{s})}{s^{1+\alpha} K_0(\sqrt{s})} = \infty$$

and we will not be able to compute the contribution of the small circumference of Bromwich's contour. Inspired in (44) we can write

$$\mathfrak{L}^{-1} \left[ \frac{1}{s^\alpha} \frac{K_0(\rho\sqrt{s})}{K_0(\sqrt{s})} \right] = \mathfrak{L}^{-1} \left[ \frac{e^{-(\rho-1)\sqrt{s}}}{\sqrt{\rho} s^\alpha} \right] + \mathfrak{L}^{-1} \left[ \frac{1}{s^\alpha} \left( \frac{K_0(\rho\sqrt{s})}{K_0(\sqrt{s})} - \frac{e^{-(\rho-1)\sqrt{s}}}{\sqrt{\rho}} \right) \right] =$$

and by formula [[11], section 5.6, formula 21]

$$\begin{aligned} &= \mathfrak{L}^{-1} \left[ \frac{1}{s^\alpha} \left( \frac{K_0(\rho\sqrt{s})}{K_0(\sqrt{s})} - \frac{e^{-(\rho-1)\sqrt{s}}}{\sqrt{\rho}} \right) \right] + \\ &+ \frac{1}{2\sqrt{\pi\rho}} \frac{1}{(\rho-1)^{\alpha-\frac{1}{2}}} \frac{1}{\xi^{\frac{3}{2}}} \int_0^\infty u^{\alpha+\frac{1}{2}} e^{-\frac{u^2}{4\xi}} J_{2\alpha-1}(2\sqrt{\rho-1}\sqrt{u}) du. \end{aligned} \quad (45)$$

We check that this new inverse Laplace transform can be computed using the Bromwich's contour of figure 2-B. If  $s \in \mathcal{D}_0$ ,  $Re(s) \leq \gamma_0$  and  $|s|$  is large enough, there is a constant  $C_7(\rho) > 0$  such that

$$\begin{aligned} &\left| \frac{1}{s^\alpha} \left( \frac{K_0(\rho\sqrt{s})}{K_0(\sqrt{s})} - \frac{e^{-(\rho-1)\sqrt{s}}}{\sqrt{\rho}} \right) \right| = \\ &= \left| \frac{1}{s^\alpha} \left( \frac{\sqrt{\frac{\pi}{2\rho\sqrt{s}}} e^{-\rho\sqrt{s}} \left( 1 + O\left(\frac{1}{\rho\sqrt{s}}\right) \right)}{\sqrt{\frac{\pi}{2\sqrt{s}}} e^{-\sqrt{s}} \left( 1 + O\left(\frac{1}{\sqrt{s}}\right) \right)} - \frac{e^{-(\rho-1)\sqrt{s}}}{\sqrt{\rho}} \right) \right| = \\ &= \frac{1}{|s|^\alpha} \left| \frac{e^{-(\rho-1)\sqrt{s}} \left( \left( 1 + O\left(\frac{1}{\rho\sqrt{s}}\right) \right) - \left( 1 + O\left(\frac{1}{\sqrt{s}}\right) \right) \right)}{\sqrt{\rho} \left( 1 + O\left(\frac{1}{\sqrt{s}}\right) \right)} \right| \leq \\ &\leq \frac{C_7(\rho)}{|s|^\alpha} \left| \frac{e^{-(\rho-1)\sqrt{s}}}{\sqrt{\rho}\sqrt{s}} \right| \leq \frac{C_7(\rho)}{\sqrt{\rho}} \frac{1}{|s|^{\alpha+\frac{1}{2}}} \end{aligned} \quad (46)$$

because  $\cos \left( \frac{Arg s}{2} \right) \geq 0$ . As  $\alpha + \frac{1}{2} > 1$  our claim is proved.

Then, since there are no singular point inside the integration contour ([[10] section 15.7]) and

$$\lim_{s \rightarrow 0, s \in \mathcal{D}_0} s \frac{e^{s\xi}}{s^\alpha} \left( \frac{K_0(\rho\sqrt{s})}{K_0(\sqrt{s})} - \frac{e^{-(\rho-1)\sqrt{s}}}{\sqrt{\rho}} \right) = 0 \quad (47)$$

by Bromwich's formula, (46), Jordan's lemma and the theorem of residues we obtain

$$\begin{aligned} h(\rho, \xi, v, \alpha) &:= \mathfrak{L}^{-1} \left[ \frac{1}{s^\alpha} \left( \frac{K_0(\rho\sqrt{s})}{K_0(\sqrt{s})} - \frac{e^{-(\rho-1)\sqrt{s}}}{\sqrt{\rho}} \right) \right] (\rho, \xi) = \\ &= \lim_{R \rightarrow \infty, \varepsilon \rightarrow 0} \frac{1}{2\pi i} \left( - \int_{L_1} \frac{e^{s\xi}}{s^\alpha} \left( \frac{K_0(\rho\sqrt{s})}{K_0(\sqrt{s})} - \frac{e^{-(\rho-1)\sqrt{s}}}{\sqrt{\rho}} \right) ds \right. \\ &\quad \left. - \int_{L_2} \frac{e^{s\xi}}{s^\alpha} \left( \frac{K_0(\rho\sqrt{s})}{K_0(\sqrt{s})} - \frac{e^{-(\rho-1)\sqrt{s}}}{\sqrt{\rho}} \right) ds \right) = \end{aligned}$$

and by (64)

$$= \frac{-1}{\pi} \text{Im} \int_{-\infty}^0 \frac{e^{s\xi} e^{-\alpha\pi i}}{(-s)^\alpha} \left( \frac{J_0(\rho\sqrt{-s}) i + Y_0(\rho\sqrt{-s})}{J_0(\sqrt{-s}) i + Y_0(\sqrt{-s})} - \frac{e^{-(\rho-1)\sqrt{-s} i}}{\sqrt{\rho}} \right) ds \quad (48)$$

and after the change  $x = -s$

$$\begin{aligned} &= -\frac{1}{\pi} \int_0^\infty \frac{e^{-x\xi}}{x^\alpha} \left( \frac{\cos(\alpha\pi)A_3(x) - \sin(\alpha\pi)A_5(x)}{J_0^2(\sqrt{x}) + Y_0^2(\sqrt{x})} \right. \\ &\quad \left. + \cos(\alpha\pi) \frac{\sin(\rho-1)\sqrt{x}}{\sqrt{\rho}} + \sin(\alpha\pi) \frac{\cos(\rho-1)\sqrt{x}}{\sqrt{\rho}} \right) dx. \quad (49) \end{aligned}$$

The same method of subsection (3.2.1) proves that (49) converges uniformly for  $\alpha \in [\frac{1}{2}, \frac{3}{4}[$ . Hence  $h(\rho, \xi, v, \alpha)$  is right continuous at  $\alpha = \frac{1}{2}$  and by (38) and (49)

$$\begin{aligned} \mathfrak{L}^{-1}[G_4](\rho, \xi, v) &= \frac{1}{\sqrt{\pi}} \int_0^\xi \frac{g_4(\rho, w, v, \frac{1}{2})}{\sqrt{\xi-w}} dw = \\ &= \frac{1}{\sqrt{\pi}} \int_0^\xi \frac{1}{\sqrt{\xi-w}} \left( h\left(\rho, w, v, \frac{1}{2}\right) + \frac{1}{2\sqrt{\pi\rho}} \frac{1}{w^{\frac{3}{2}}} \int_0^\infty u e^{-\frac{u^2}{4w}} J_0(2\sqrt{(\rho-1)u}) du \right) dw = \\ &\quad (50) \\ &= \frac{1}{\sqrt{\pi^3}} \int_0^\xi \frac{1}{\sqrt{\xi-w}} \left( \int_0^\infty \frac{e^{-x\xi}}{\sqrt{x}} \left( \frac{J_0(\sqrt{x})J_0(\rho\sqrt{x}) + Y_0(\sqrt{x})Y_0(\rho\sqrt{x})}{J_0^2(\sqrt{x}) + Y_0^2(\sqrt{x})} - \frac{\cos(\rho-1)\sqrt{x}}{\sqrt{\rho}} \right) dx \right. \\ &\quad \left. + \frac{1}{2\sqrt{\pi\rho}} \frac{1}{w^{\frac{3}{2}}} \int_0^\infty u e^{-\frac{u^2}{4w}} J_0(2\sqrt{(\rho-1)u}) du \right) dw. \end{aligned}$$

### 3.2.5 Complete solution

As a consequence of previous results it follows from (33)

$$\begin{aligned}
V(\rho, \xi) = & \frac{1}{2\sqrt{\pi}} \int_1^\infty \frac{1}{v} \left( \int_0^\infty \left( \int_0^\xi \frac{e^{-xw}}{\sqrt{\xi-w}} dw \right) \frac{1}{\sqrt{x}} \left( -Y_0(v\sqrt{x})J_0(\rho\sqrt{x}) \right) dx \right) dv + \\
& + \frac{1}{2\sqrt{\pi}} \int_1^\infty \frac{1}{v} \left[ \int_0^\infty \left( \int_0^\xi \frac{e^{-xw}}{\sqrt{\xi-w}} dw \right) \frac{1}{\sqrt{x}} \times \right. \\
& \left. \left( J_0(\sqrt{x})Y_0(v\sqrt{x}) \frac{J_0(\rho\sqrt{x})J_0(\sqrt{x}) + Y_0(\sqrt{x})Y_0(\rho\sqrt{x})}{J_0^2(\sqrt{x}) + Y_0^2(\sqrt{x})} \right. \right. \\
& \left. \left. - J_0(v\sqrt{x})J_0(\sqrt{x}) \frac{J_0(\rho\sqrt{x})Y_0(\sqrt{x}) - J_0(\sqrt{x})Y_0(\rho\sqrt{x})}{J_0^2(\sqrt{x}) + Y_0^2(\sqrt{x})} \right) dx \right] dv \\
& - \frac{B}{\sqrt{\pi^3}} \int_0^\infty \left( \int_0^\xi \frac{e^{-xw}}{\sqrt{\xi-w}} \right) \left( \frac{J_0(\sqrt{x})J_0(\rho\sqrt{x}) + Y_0(\sqrt{x})Y_0(\rho\sqrt{x})}{\sqrt{x}(J_0^2(\sqrt{x}) + Y_0^2(\sqrt{x}))} - \frac{\cos(\rho-1)\sqrt{x}}{\sqrt{\rho}\sqrt{x}} \right) dx \\
& - \frac{B}{2\pi^2\sqrt{\rho}} \int_0^\xi \frac{1}{\sqrt{\xi-w}} \frac{1}{w^{\frac{3}{2}}} \left( \int_0^\infty u e^{-\frac{u^2}{4w}} J_0(2\sqrt{(\rho-1)u}) du \right) dw. \quad (51)
\end{aligned}$$

### 3.2.6 Behavior when time tends to infinitum

Let us see that for large values of  $\xi$

$$V(\rho, \xi) \geq \frac{e}{\pi} \log^2(2\sqrt{\xi}) - M_8(\rho) \quad (52)$$

for some  $M_8(\rho) > 0$  independent of  $\xi$ . Then  $\lim_{\xi \rightarrow \infty} V(\rho, \xi) = \infty$  whatever  $\rho > 1$  is and (52) will give the order of magnitude of  $V(\rho, \xi)$ .

The rigorous proof is quite long. A simple look at (51) and Fubini's theorem shows that  $V(\rho, \xi)$  can be expressed as  $V(\rho, \xi) = \sum_{j=1}^4 V_j(\rho, \xi)$  where

$$V_j(\rho, \xi) = \int_1^\infty \left( \int_0^\infty f_j(x, v) \left( \int_0^\xi \frac{e^{-xw}}{\sqrt{\xi-w}} dw \right) dx \right) dv \quad j = 1, 2,$$

$$V_3(\rho, \xi) = - \int_0^\infty f_3(x, v) \left( \int_0^\xi \frac{e^{-xw}}{\sqrt{\xi-w}} dw \right) dx, \quad V_4(\rho, \xi) = - \int_0^\xi \frac{f_4(w)}{\sqrt{\xi-w}} dw$$

for certain functions  $f_j(x, v)$ ,  $1 \leq j \leq 3$  and  $f_4(w)$ .

We make a detailed analysis of  $V_1(\rho, \xi)$ . For fixed  $\rho > 1$  and  $\xi > 0$ , using Fubini's theorem and doing the change  $v\sqrt{x} = \theta$ , for every  $M > \frac{1}{\xi}$  one has

$$V_1(\rho, \xi) = \int_0^\infty \frac{J_0(\rho\sqrt{x})}{\sqrt{x}} \left( \int_0^\xi \frac{e^{-xw}}{\sqrt{\xi-w}} dw \right) \left( \int_1^\infty -\frac{Y_0(v\sqrt{x})}{v} dv \right) dx =$$



$$\begin{aligned}
&= \int_0^\infty \frac{J_0(\rho\sqrt{x})}{\sqrt{x}} \left( \int_0^\xi \frac{e^{-xw}}{\sqrt{\xi-w}} dw \right) \left( \int_{\sqrt{x}}^\infty -\frac{Y_0(\theta)}{\theta} d\theta \right) dx = \\
&= \int_0^{\frac{1}{\xi}} \frac{J_0(\rho\sqrt{x})}{\sqrt{x}} \left( \int_0^\xi \frac{e^{-xw}}{\sqrt{\xi-w}} dw \right) \mathfrak{f}(x) dx + \int_{\frac{1}{\xi}}^M \frac{J_0(\sqrt{x})}{\sqrt{x}} \left( \int_0^\xi \frac{e^{-xw}}{\sqrt{\xi-w}} dw \right) \mathfrak{f}(x) dx + \\
&\quad + \int_M^\infty \frac{J_0(\rho\sqrt{x})}{\sqrt{x}} \left( \int_0^\xi \frac{e^{-xw}}{\sqrt{\xi-w}} dw \right) \mathfrak{f}(x) dx, \tag{53}
\end{aligned}$$

where  $\mathfrak{f}(x)$  is defined in the Appendix.

If  $\xi > 0$  is large enough in order that  $J_0(\rho\sqrt{x}) \geq \frac{1}{2}$  and (80) holds in  $]0, \frac{1}{\xi}]$  we obtain

$$\begin{aligned}
\int_0^{\frac{1}{\xi}} \frac{J_0(\rho\sqrt{x})}{\sqrt{x}} \left( \int_0^\xi \frac{e^{-xw}}{\sqrt{\xi-w}} dw \right) \mathfrak{f}(x) dx &\geq \int_0^{\frac{1}{\xi}} \frac{1}{4\pi} \sqrt{\xi} \left( \int_0^\xi \frac{e}{\sqrt{\xi-w}} dw \right) \log^2(2\sqrt{\xi}) dx \geq \\
&= \int_0^{\frac{1}{\xi}} \frac{e}{2\pi} \sqrt{\xi} \sqrt{\xi} \log^2(2\sqrt{\xi}) dx = \frac{e}{2\pi} \log^2(2\sqrt{\xi}). \tag{54}
\end{aligned}$$

Moreover, after the variable change  $\xi - w = \theta$ , the function

$$g(x, \xi) := \int_0^\xi \frac{e^{-xw}}{\sqrt{\xi-w}} dw = e^{-x\xi} \int_0^\xi \frac{e^{x\theta}}{\sqrt{\theta}} d\theta$$

is a decreasing function of  $x$  for every  $\xi > 0$ . In fact,

$$\frac{\partial g}{\partial x} = e^{-x\xi} \left( -\xi \int_0^\xi \frac{e^{x\theta}}{\sqrt{\theta}} d\theta + \int_0^\xi \sqrt{\theta} e^{x\theta} d\theta \right) = e^{-x\xi} \int_0^\xi e^{x\theta} \frac{\theta - \xi}{\sqrt{\theta}} d\theta < 0.$$

It follows that

$$\forall x \in \left[ \frac{1}{\xi}, \infty \right[ \quad 0 \leq g(x, \xi) \leq g\left(\frac{1}{\xi}, \xi\right) = \frac{1}{e} \int_0^\xi \frac{e^{\frac{\theta}{\xi}}}{\sqrt{\theta}} d\theta. \tag{55}$$

Now with the change  $\frac{\theta}{\xi} = \eta$  we obtain

$$\begin{aligned}
\frac{d}{d\xi} g\left(\frac{1}{\xi}, \xi\right) &= \frac{1}{e} \left( \frac{e}{\sqrt{\xi}} - \frac{1}{\xi^2} \int_0^\xi \sqrt{\theta} e^{\frac{\theta}{\xi}} d\theta \right) = \frac{1}{e} \left( \frac{e}{\sqrt{\xi}} - \frac{\xi^{\frac{3}{2}}}{\xi^2} \int_0^1 \sqrt{\eta} e^\eta d\eta \right) = \\
&= \frac{1}{e\sqrt{\xi}} \left( e - \int_0^1 \sqrt{\eta} e^\eta d\eta \right) < \frac{1}{e\sqrt{\xi}} \left( e - \int_0^1 \sqrt{\eta} d\eta \right) < 0,
\end{aligned}$$

that is,  $g\left(\frac{1}{\xi}, \xi\right)$  is decreasing with respect to  $\xi$  and so

$$\forall \xi \geq 1 \quad g\left(\frac{1}{\xi}, \xi\right) \leq g(1, 1). \tag{56}$$

Let  $M > 0$  be large enough so that the asymptotic expansions (67), (68) and (81) hold. Then, there is  $M_1(\rho) > 0$  (independent of  $\xi$  and  $x$ ) such that by (55) and (56)

$$\begin{aligned} & \forall \xi \geq 1 \quad \left| \int_M^\infty \frac{J_0(\rho\sqrt{x})}{\sqrt{x}} \left( \int_0^\xi \frac{e^{-xw}}{\sqrt{\xi-w}} dw \right) f(x) dx \right| \leq \\ & \leq M_1(\rho) \int_M^\infty \frac{1}{\sqrt[4]{x}} \frac{1}{\sqrt{x}} g\left(\frac{1}{\xi}, \xi\right) \frac{1}{\sqrt[4]{x}} \frac{1}{\sqrt{x}} dx \leq M_1(\rho) g(1, 1) \int_M^\infty \frac{dx}{x^{\frac{3}{2}}} < \infty. \end{aligned} \quad (57)$$

Finally, by (79) there is  $M_2 > 0$  independent of  $\xi$  and  $x$  such that

$$\begin{aligned} & \left| \int_{\frac{1}{\xi}}^M \frac{J_0(\rho\sqrt{x})}{\sqrt{x}} \left( \int_0^\xi \frac{e^{-xw}}{\sqrt{\xi-w}} dw \right) f(x) dx \right| \leq g(1, 1) \int_{\frac{1}{\xi}}^M \left| \frac{J_0(\rho\sqrt{x})}{\sqrt{x}} f(x) \right| dx \leq \\ & \leq M_2 g(1, 1) \int_{\frac{1}{\xi}}^M \left| \frac{J_0(\rho\sqrt{x})}{\sqrt{x}} \log^2\left(\frac{\sqrt{x}}{2}\right) \right| dx \leq \\ & \leq M_2 g(1, 1) \int_0^M \left| \frac{J_0(\rho\sqrt{x})}{\sqrt{x}} \log^2\left(\frac{\sqrt{x}}{2}\right) \right| dx < \infty, \end{aligned} \quad (58)$$

the last integral being convergent by (59).

With analogous arguments but using (75) and (74) it can be proved that  $V_2(\rho, \xi)$  has a decomposition in the sum of three summands verifying the same type of **upper and lower bounds**. Hence by (54), (57) and (58) we obtain

$$|V_1(\rho, \xi) + V_2(\rho, \xi)| \geq \frac{e}{2\pi} \log^2(2\sqrt{\xi}) - M_3(\rho)$$

for some  $M_3(\rho) > 0$  independent of  $\xi$ .

With respect to  $V_3(\rho, \xi)$ , by the oscillatory character of Bessel functions  $J_0(x)$  and  $Y_0(x)$  there are  $M_4(\rho) > 0$ ,  $M_5 > 0$ ,  $M_6(\rho) > 0$  and  $x_0 > 0$  such that

$$\begin{aligned} |V_3(\rho, \xi)| & \leq M_4(\rho) \int_0^{\frac{1}{\xi}} \int_0^\xi \left( \frac{dw}{\sqrt{\xi-w}} \right) \frac{dx}{\sqrt{x}} + M_5 g(1, 1) \left| \int_{\frac{1}{\xi}}^{x_0} f_3(x) dx \right| \leq \\ & \leq 4 M_4(\rho) \sqrt{\xi} \frac{1}{\sqrt{\xi}} + M_6(\rho). \end{aligned}$$

To finish, with the change  $u = 2\sqrt{w} \eta$  we obtain

$$|V_4(\rho, \xi)| \leq M_7(\rho) \left| \int_0^\xi \frac{4 dw}{\sqrt{\xi-w}\sqrt{w}} \int_0^\infty \eta e^{-\eta^2} J_0(2\sqrt{2(\rho-1)\sqrt{w}\eta}) d\eta \right| \leq$$

for some  $M_7(\rho) > 0$  and with another change  $w = \eta\theta$

$$\leq 4 M_7(\rho) \int_0^1 \frac{d\theta}{\sqrt{1-\theta}\sqrt{\theta}} \int_0^\infty \eta e^{-\eta^2} d\eta < \infty.$$

Putting together these partial results we obtain the expression of Eq. (52).

### 3.3 Plotting results

We obtained full expressions of the analytical solutions of temperature at any time and in any spatial domain. Unfortunately, we were not able to plot them (Eq. (20) and (51)) with our available computing resources (Mathematica 8.0 software, Wolfram Research Inc., Champaign, IL, USA) except when a steady-state is reached (Eq. (19)) due to the plotting task being extremely time-consuming. For this reason, and only to illustrate graphically some of the conclusions related to thermal behavior, we employed the COMSOL Multiphysics software (COMSOL, Burlington MA, USA) to plot Figures 3 and 4. To do this, we have to particularize the following model parameters: Blood temperature and the initial tissue temperature  $T_b = T_0 = 37^\circ\text{C}$ , radius of the electrode  $r_0 = 1.5 \text{ mm}$ , boundary temperature  $T_C = 5^\circ\text{C}$ , current density  $j_0 = 3.5 \text{ mA/mm}^2$ , electrical conductivity  $\sigma = 0.33 \text{ S/m}$ , thermal conductivity  $k = 0.502 \text{ W/(m K)}$ , density  $\eta = 1060 \text{ kg/m}^3$  and specific heat  $c = 3600 \text{ J/(kg K)}$ .

Figure 3 shows the time progresses of the temperature profiles for four values of  $R$  (0.1, 0.5, 1.0 and 2.0 m) and five values of time  $t$  (60 s, 6 min, 1 hour, 10 hours, 100 hours). The choose of so large values for  $R$  and  $t$  is justified since we are interested in to visualize the behavior of the temperature when  $R$  and  $t$  tend to infinitum. The temperature limit is also plotted (following equation (19)). It is noticeable that the convergence toward the limit is very slow compared to the typical durations used in RF ablation (12 minutes). **Figure 3 also explains why the temperature is not so well controlled when blood supply is blocked during surgery, in contrast what happens when the perfusion term is considered [7].**

Figure 4 shows the temperature profiles computed at a specific time (720 s and 8000 s) for different values of the spatial domain ( $R$ ). The abscissas axis is normalized ( $r/R$ ) in order to compare simultaneously all the cases. Note that from  $R = 50 \text{ cm}$  on, **the graphics seems to tend towards a certain profile, and it is reasonable to think this profile is the plot of the solution analytically obtained with the boundary condition at infinity (Equation (51)) which cannot be plotted with our computing resources. Moreover, Figure 4 could conceivably be used as a guideline in design of clinical implementation.**

## 4 Discussion

In this study we obtained the analytical solution for the temperature distribution in the tissue for any time during RFA with an internally cooled needle-like electrode when the blood perfusion term is not included in the governing equation.

We obtained the full expressions in two cases: when the boundary condition of the placement of the dispersive electrode was mathematically assumed to be at infinity, and when this boundary condition was mathematically assumed to be at a finite distance  $R$ . The first approach has traditionally been used in analytical modeling studies on RF heating of biological tissues, while the second is obligatorily employed in numerical models (e.g. infinite element models) since the model domain has of necessity to be limited. As far as we know this is the first attempt to solve these problems analytically.

Although Haemmerich et al [3] previously focused on this same analytical problem, they only solved the steady-state solution. This study is a natural extension of previous work in which we solved the RFA thermal problem in biological tissues analytically when the blood perfusion term was included in the governing equation [7]. The case of the infinite spatial domain, which is only significant from a mathematical point of view, would allow us to understand the thermal performance at points both near and far from the electrode. However, we also noticed that the method of obtaining the analytical solution had to be drastically different when the blood perfusion term (see Eq. 1) was zero. Setting this parameter to zero involves modeling the RFA of an organ in which atraumatic vascular clamping has been conducted to temporally interrupt blood perfusion so as to achieve larger thermal lesions. Consequently, the specific case of the general solution remained unsolved. We initially thought that the solution without the blood perfusion term would be qualitatively similar to that reported in [7], since the solution frequently depends continuously on the parameters. Surprisingly, we found out that: 1) the lack of the blood perfusion term not only modified the method of the solution, but also, and more importantly, the temperature distribution; and 2) the spatial domain was a critical factor. In short, in bounded spatial domains, the temperature reaches a steady-state, for example in a real situation, since it is known that all monopolar RF ablation involves a dispersive electrode placed no further than 1 meter from the active electrode. But, if the spatial domain is potentially infinite (boundary condition set at infinitum), temperature increases over time without reaching a steady-state. This confirms the strong dependence on the model with the spatial domain dimension and suggests that in a problem with a realistic (finite) dimension, the solving process using numerical methods makes it necessary to carefully choose the best spatial domain dimension. All this is certainly interesting and clearly different from existing mathematical models of spherical electrodes, in which the limit temperature is always reached, in both the finite and infinite domains [12]. We think that the reason is that while the power deposited in the tissue ( $W/m^3$ ) decays at  $1/r^4$  around a spherical electrode, i.e. relatively fast, it does so at  $1/r^2$  around cylindrical electrodes, which implies that power deposition is less circumscribed in the case of cylindrical electrodes and temperatures are higher at a distance from the electrode.

## 4.1 Practical implications

This analytical modeling study included important simplifications. This means that the clinical implications are few, as opposed to numerical models, which include realistic geometries and a fine characterization of biological tissues. In spite of this, analytical solutions represent exact solutions to the mathematical framework that underlies physical problems, and therefore deserve to be analyzed in detail in order to study their performance. We think that our findings are interesting not only for future analytical models, but also for numerical models involving cylindrical electrodes for RF heating of biological tissues. For instance, the existence of a temperature limit when a finite domain is considered could justify some simplifications in future numerical models in order to create predictive models with undemanding computing requirements. Transient analysis are highly time-consuming, and the possibility of directly computing the limit temperature could allow fast predictions of the outcome of an RF ablation in terms of thermal lesion size.

## 4.2 Limitations of the study

Although we were not able to plot the temperature profiles directly from the obtained analytical expression, we could analytically demonstrate the behavior of the temperature profiles depending on the considered time and spatial domain considered. As in previous analytical models, we do not consider the temperature-dependence of the electrical and thermal characteristics of the tissue, especially the drastic drop in electrical conductivity when temperature reaches 100°C (associated with tissue desiccation). The reason is that these changes would imply a non linear equation, which cannot be analytically solved. This means that in a real situation the electrical-thermal performance could be a slightly different if tissue temperature reaches values around 100°C. Phenomena of desiccation and eventually carbonization would limit the growth of the thermal lesion.

## Appendix: Results about Bessel functions

To solve the initial boundary value problem (24), (25), (26), (27) we shall need some specific elementary computations as well an intensive use of well known deep properties of Bessel and modified Bessel functions of complex argument. We present here all of them in order to make the text clearer.

a) *Some elementary results.* Given  $a > 0, b > 0$ , by L'Hôpital's rule

$$\lim_{x \rightarrow 0} x^a \log(b\sqrt{x}) = \lim_{x \rightarrow 0} -\frac{x^{a+1}}{2\sqrt{x}\sqrt{x}} = \lim_{x \rightarrow 0} -\frac{x^a}{2a} = 0 \quad (59)$$

and

$$\lim_{x \rightarrow 0} \frac{\log \frac{a\sqrt{x}}{2}}{\log \frac{b\sqrt{x}}{2}} = 1. \quad (60)$$

b) *Series expansions of Bessel function  $Y_0(z)$  and  $K_0(z)$ .* One has

$$Y_0(z) = \frac{2}{\pi} \left( J_0(z) \log \left( \frac{z}{2} \right) - \sum_{m=0}^{\infty} (-1)^m \frac{\psi(m+1)}{2^{2m}(m!)^2} z^{2m} \right) \quad (61)$$

and

$$K_0(z) = -I_0(z) \log \left( \frac{z}{2} \right) + \sum_{m=0}^{\infty} \frac{\psi(m+1)}{2^{2m}(m!)^2} z^{2m}, \quad (62)$$

where  $\psi(1) = -\gamma$ ,  $\psi(m+1) = 1 + \frac{1}{2} + \frac{1}{3} + \dots + \frac{1}{m} - \gamma$  and  $\gamma$  is the Euler-Mascheroni constant, which implies that

$$K_0(z) = -I_0(z) \log \left( \frac{z}{2} \right) + Z(z), \quad (63)$$

where  $Z(z)$  is an even holomorphic function on  $\mathbb{C}$

c) *Some relations between Bessel functions used in the text.* By [[14], 9.6.4 and 9.1.4]

$$\forall z \in \mathbb{C} \quad \frac{\pi}{2} < \arg(z) \leq \pi \quad K_0(z) = -\frac{\pi}{2} (J_0(-z i) i + Y_0(-z i)) \quad (64)$$

and by [[14], 9.1.40 and 9.6.32 and ]

$$\forall z \in \mathcal{D}_0 \quad J_0(\bar{z}) = \overline{J_0(z)}, \quad Y_0(\bar{z}) = \overline{Y_0(z)}, \quad K_0(\bar{z}) = \overline{K_0(z)} \quad (65)$$

Moreover,

$$\forall z \in \mathbb{C} \quad I_0(z) = J_0(z i) \quad (66)$$

d) *Asymptotic expansions of some Bessel functions.* For  $x \rightarrow \infty$  in  $\mathbb{R}$  one has the asymptotic expansions ([14], 9.2.1 and 9.2.2]

$$J_0(x) \sim \sqrt{\frac{2}{\pi x}} \cos \left( x - \frac{\pi}{4} \right) + O \left( \frac{1}{x} \right) \quad (67)$$

and

$$Y_j(x) \sim \sqrt{\frac{2}{\pi x}} \sin \left( x - \frac{j\pi}{2} - \frac{\pi}{4} \right) + O \left( \frac{1}{x} \right), \quad j = 0, 1. \quad (68)$$

It follows that

$$J_0^2(x) + Y_0^2(x) \sim \frac{2}{\pi x} + O \left( \frac{1}{x^{\frac{3}{2}}} \right) \quad (69)$$

and, for  $a > 0, b > 0$ , after elementary operations and inequalities

$$\begin{aligned} & \left| \frac{J_0(a\sqrt{x})J_0(b\sqrt{x}) \pm Y_0(b\sqrt{x})Y_0(a\sqrt{x})}{J_0^2(\sqrt{x}) + Y_0^2(\sqrt{x})} \right| = \\ & = \left| \frac{\frac{2}{\pi\sqrt{abx}} \cos\left((a \mp b)\sqrt{x} - \frac{\pi}{4} \pm \frac{\pi}{4}\right) + O\left(\frac{1}{b\sqrt{ax}^{\frac{3}{4}}}\right)}{\frac{2}{\pi\sqrt{x}} + O\left(\frac{1}{x^{\frac{3}{4}}}\right)} \right| < \infty. \end{aligned} \quad (70)$$

With respect to modified Bessel functions, one has the following asymptotic expansions for  $|z| \rightarrow \infty$  and  $\nu \in \mathbb{N} \cup \{0\}$  (see [[10], 7.2.3]):

$$I_\nu(z) \sim \frac{e^z}{\sqrt{2\pi z}} \left(1 + O\left(\frac{1}{z}\right)\right) + \frac{e^{-z+(\nu+\frac{1}{2})\pi i}}{\sqrt{2\pi z}} \left(1 + O\left(\frac{1}{z}\right)\right) \quad \text{if } -\frac{\pi}{2} < \text{Arg}(z) < \frac{3\pi}{2}, \quad (71)$$

$$I_\nu(z) \sim \frac{e^z}{\sqrt{2\pi z}} \left(1 + O\left(\frac{1}{z}\right)\right) + \frac{e^{-z-(\nu+\frac{1}{2})\pi i}}{\sqrt{2\pi z}} \left(1 + O\left(\frac{1}{z}\right)\right) \quad \text{if } -\frac{3\pi}{2} < \text{Arg}(z) < \frac{\pi}{2} \quad (72)$$

and

$$K_0(z) \sim \sqrt{\frac{\pi}{2z}} e^{-z} \left(1 + O\left(\frac{1}{z}\right)\right) \quad \text{if } |\text{Arg}(z)| \leq \frac{3\pi}{2} \quad (73)$$

As an application of previous expansions, if  $a > 0, b > 0$  and  $x > 0$ , by (63) and (60)

$$\left| \frac{J_0(a\sqrt{x}) - Y_0(a\sqrt{x})}{J_0(b\sqrt{x}) - Y_0(b\sqrt{x})} i \right| = \left| \frac{\log \frac{a\sqrt{x}}{2} - I_0(a\sqrt{x}) + \frac{Z(a\sqrt{x})}{\log \frac{a\sqrt{x}}{2}} \frac{J_0(a\sqrt{x})}{Y_0(a\sqrt{x})} - i}{\log \frac{b\sqrt{x}}{2} - I_0(b\sqrt{x}) + \frac{Z(b\sqrt{x})}{\log \frac{b\sqrt{x}}{2}} \frac{J_0(b\sqrt{x})}{Y_0(b\sqrt{x})} - i} \right| < \infty. \quad (74)$$

e) Asymptotic expansions of some integrals. By [[14], 11.1.20] we have

$$\int_{\sqrt{x}}^{\infty} \frac{J_0(t)}{t} dx = -\gamma - \log \frac{\sqrt{x}}{2} + \sum_{k=1}^{\infty} \frac{(-1)^{k+1} \left(\frac{\sqrt{x}}{2}\right)^{2k}}{2k(k!)^2} \quad (75)$$

as well as the formula [[14], 11.1.21]

$$\mathfrak{f}(x) := \int_{\sqrt{x}}^{\infty} -\frac{Y_0(t)}{t} dx = \mathfrak{f}_1(x) + \mathfrak{f}_2(x) \quad (76)$$

where

$$\mathfrak{f}_1(x) = \frac{1}{\pi} \log^2 \left(\frac{\sqrt{x}}{2}\right) + \frac{2\gamma}{\pi} \log \left(\frac{\sqrt{x}}{2}\right) - \frac{1}{\pi} \left(\frac{\pi^2}{6} - \gamma^2\right) \quad (77)$$

and

$$f_2(x) = \frac{2}{\pi} \sum_{k=1}^{\infty} \frac{(-1)^{k+1} \left(\frac{\sqrt{x}}{2}\right)^{2k}}{2k(k!)^2} \left( \psi(k+1) + \frac{1}{2k} - \log \frac{\sqrt{x}}{2} \right). \quad (78)$$

Then

$$f(x) = \log^2 \left( \frac{\sqrt{x}}{2} \right) \left( \frac{1}{\pi} + \frac{\frac{2\gamma}{\pi} \log \left( \frac{\sqrt{x}}{2} \right) - \frac{1}{\pi} \left( \frac{\pi^2}{6} - \gamma^2 \right) + f_2}{\log^2 \left( \frac{\sqrt{x}}{2} \right)} \right) \quad (79)$$

and taking  $\xi > 0$  large enough we obtain

$$\forall x \in \left] 0, \frac{1}{\xi} \right] \quad f(x) \geq \frac{1}{2\pi} \log^2 \frac{1}{2\sqrt{\xi}} = \frac{1}{2\pi} \log^2(2\sqrt{\xi}). \quad (80)$$

Finally, we shall need the asymptotic expansion of  $f(x)$  for  $x \rightarrow \infty$  deduced from [[14], 11.1.24]

$$f(x) \sim Y_1(\sqrt{x}) \frac{1}{\sqrt{x}} \left( 1 + O\left(\frac{1}{x}\right) \right) - \frac{2}{x} Y_0(\sqrt{x}) \left( 1 + O\left(\frac{1}{x}\right) \right) \quad (81)$$

**Financial support:** This work received financial support from the Spanish "Plan Estatal de Investigación, Desarrollo e Innovación Orientada a los Retos de la Sociedad" under Grant TEC2014-52383-C3-R (TEC2014-52383-C3-1-R).

## References

- [1] B. L. Yun, J. M. Lee, J. H. Baek, S. H. Kim, J. Y. Lee, J. K. Han, B. I. Choi, Radiofrequency ablation for treating liver metastases from a non-colorectal origin, *Korean Journal of Radiology*, 12 (5) (2011) 579-587.
- [2] A. Erez, A. Shitzer, Controlled destruction and temperature distributions in biological tissues subjected to monoactive electroagulation, *Journal of Biomechanical Engineering* 102 (1980) 42-49.
- [3] D. Haemmerich, L. Chachati, A. S. Wright, D. M. Mahvi, F. T. Jr. Lee, J. G. Webster, Hepatic radiofrequency ablation with internally cooled probes: effect of coolant temperature on lesion size, *IEEE Transactions on Biomedical Engineering*, 50 (4) (2003) 493-500, April 2003.
- [4] J. D. Wiley, and J. G. Webster, Analysis and control of the current distribution under circular dispersive electrodes, *IEEE Transactions on Biomedical Engineering* 29 (1982) 381-385.



- [5] K. M. Overmyer, J. A. Pearce, D. P. de Witt, Measurements of temperature distributions at electro-surgical dispersive electrode sites, *Transactions of the ASME, Journal of Biomechanical Engineering* 101 (1976) 66-72.
- [6] D. E. Haines, D. D. Watson, Tissue heating during radiofrequency catheter ablation: a thermodynamic model and observations in isolated perfused and superfused canine right ventricular free wall, *Pacing and Clinical Electrophysiology*, 12 (1989) 962-967.
- [7] J. A. López Molina, M. J. Rivera, E. J. Berjano, Analytical model based on a cylindrical geometry to study of RF ablation with needle-like internally cooled electrode, *Mathematical Problems in Engineering*, Article ID 834807, 16 pages, (2012).
- [8] D. J. Scott, J. B. Fleming, L. M. Watumull, G. Lindberg, S. T. Tesfay, D. B. Jones, The effect of hepatic inflow occlusion on laparoscopic radiofrequency ablation using simulated tumors, *Surgical Endoscopy*, 16 (9) (2002) 1286-91.
- [9] E. J. Berjano, Theoretical modeling for radiofrequency ablation: state-of-the-art and challenges for the future, *BioMedical Engineering OnLine* 18 (2006) 5-24.
- [10] G. N. Watson, *A treatise on the theory of Bessel functions*, Cambridge Mathematical Library, Cambridge University Press, Cambridge, (1995).
- [11] A. Erdélyi, W. Magnus, F. Oberhettinger, F. G. Tricomi, *Tables of integral transforms*, Vol. II, McGraw-Hill Book Company Inc., New York, (1954)
- [12] J. A. López Molina, M. J. Rivera, E. J. Berjano, Electrical-thermal analytical modeling of monopolar RF electrocoagulation of biological tissues: impact of the blood perfusion term on the maximum temperature reached, *Mathematical Biosciences and Engineering*, 13 (2) (2016) 281-301.
- [13] S. K. Kim, H. K. Lim, J. A. Ryu, D. Choi, W. J. Lee, J. Y. Lee, J. H. Lee, Y. M. Sung, E. Y. Cho, S. M. Hong, J. S. Kim, Radiofrequency ablation of rabbit liver in vivo: effect of the pringle maneuver on pathologic changes in liver surrounding the ablation zone, *Korean Journal of Radiology* 5 (4) (2004) 240-249.
- [14] M. Abramowitz I. A. Stegun, *Handbook of mathematical functions*, U. S. Government Printing Office, Washington, (1972).

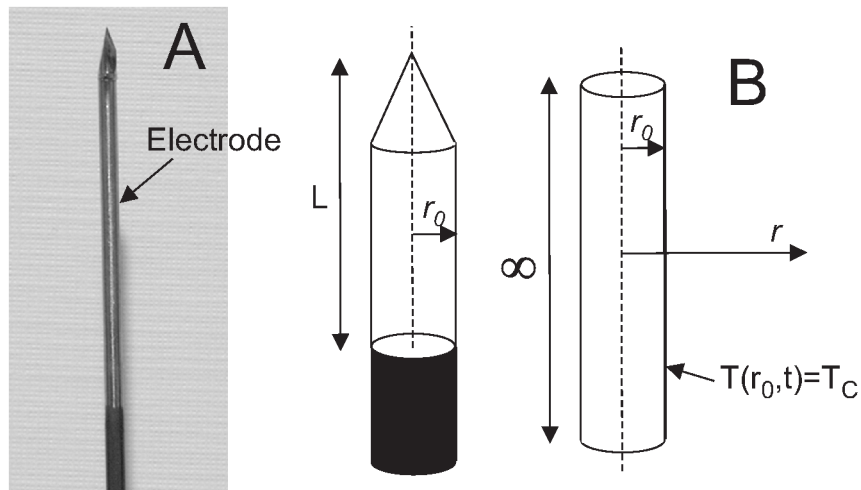


Figure 1. A: Needle-like electrode used to ablate biological tissues by means of RF currents. B: Analytical model representing a simplified scenario of an ideal conductor with infinite length totally immersed in homogeneous tissue. The internal cooling was modeled by means a Dirichlet thermal boundary condition, in particular, with a constant temperature ( $T_C$ ) which corresponds with the coolant temperature flowing inside the electrode. Accordingly, the theoretical model has one dimension ( $1D$ ), i.e. axis  $r$ .

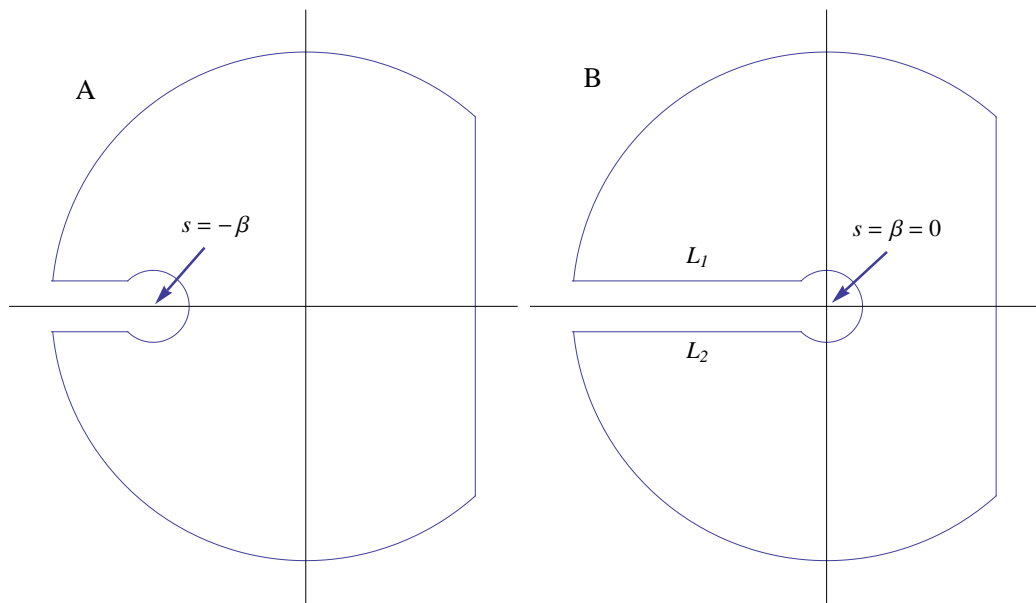


Figure 2. Bromwich's integration contours used to solve analytically the heat transfer equation with (A) and without (B) the blood perfusion term. Note that in the case with the blood perfusion term ( $\beta \neq 0$ )  $s = 0$  is not a branch point of  $D(\rho, s, \beta)$ , while in the case without blood perfusion term ( $\beta = 0$ )  $s = 0$  is a branch point of  $D(\rho, s, 0)$ .

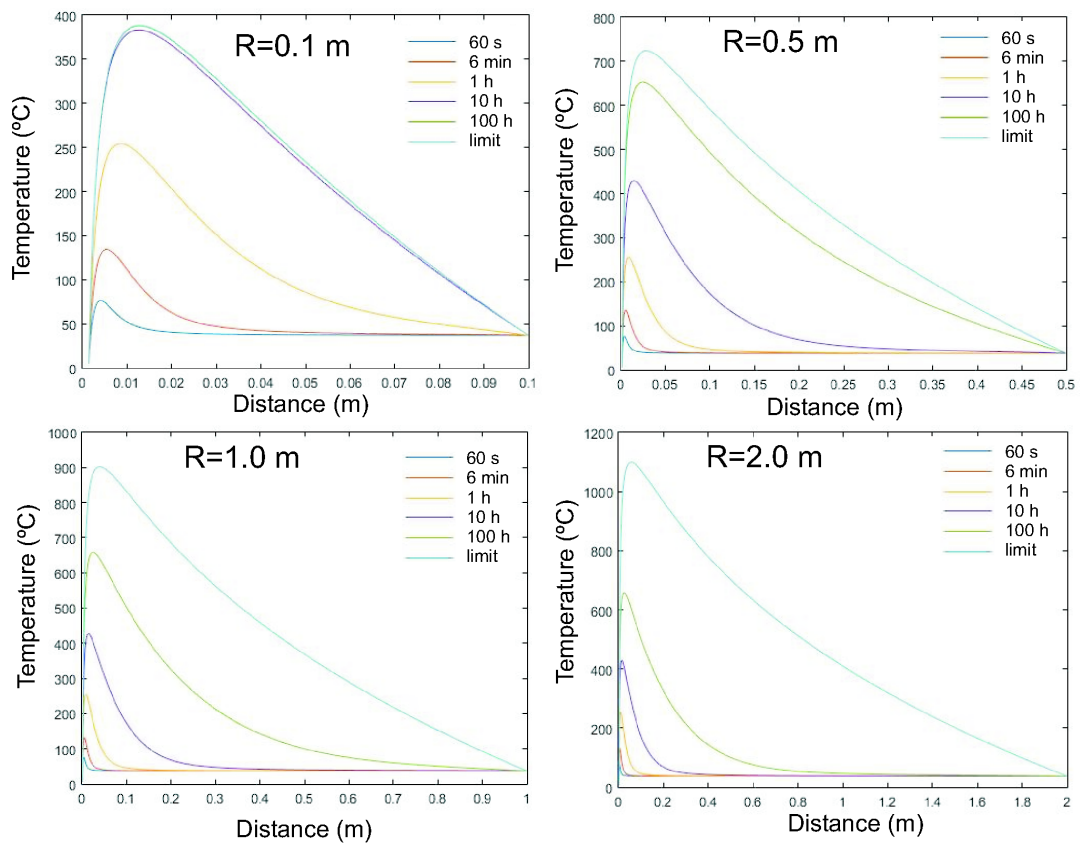


Figure 3. Time progress of the temperature profile for the case of finite domain  $R = 0.1$  m,  $R = 0.5$  m,  $R = 1$  m and  $R = 2$  m.

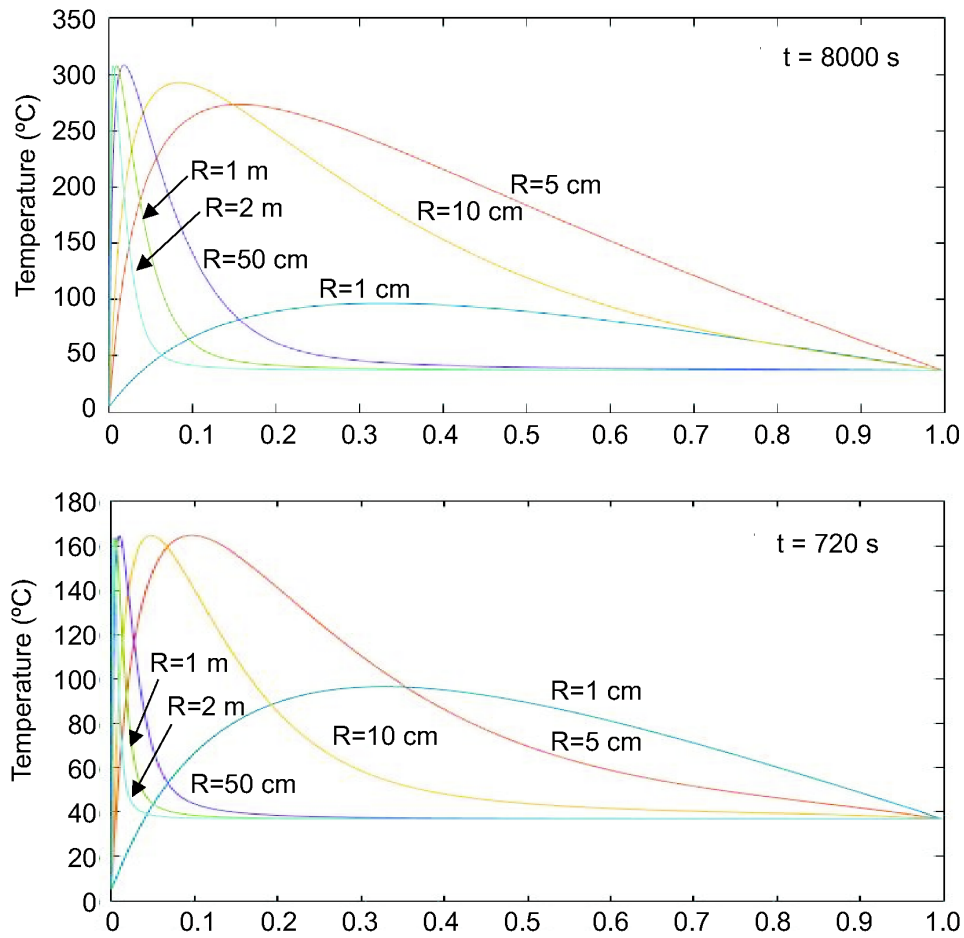


Figure 4. Temperature profiles computed at 8000 s and 720 s (typical duration of a radiofrequency ablation with a needle-like cooled electrode) for different values of the spatial domain ( $R$ ). Note that abscissas axis is normalized ( $r/R$ ).